

INTEGRATING A HUMAN THERMO-PHYSIOLOGY MODEL WITH A BUILDING SIMULATION TOOL FOR BETTER OCCUPANT REPRESENTATION.

M. Rida¹, N. Kelly¹ and A. Cowie¹

¹ Mechanical and Aerospace Engineering, University of Strathclyde, UK, Glasgow

ABSTRACT

A multi-segment thermo-physiology model was developed based on the AUB model (Salloum et al. 2007) and combined with the ESP-r building simulation tool and its integrated CFD. This enables explicit simulation of the dynamic local heat balance and thermal comfort of building occupants, within a well established building simulation environment.

At each simulation time step, the thermo-physiology model takes local environmental conditions, calculates occupant skin and core temperatures, and returns heat and moisture generation from the occupant.

The approach was demonstrated by two case studies, showing good agreement with experimental results and demonstrating effects on building performance.

1. INTRODUCTION

Simulation of energy performance in buildings often relies on simplistic underpinning assumptions with regards to heat gains from occupants and indoor conditions, with heat and moisture gains from occupants often been treated as a fixed profile, and indoor air being regarded as well mixed at a uniform temperature. Whilst this level of simplification can be useful when modelling whole building energy performance over large time scales, it has limitations particularly when analysing thermal comfort. For example, in the case of displacement ventilation, ASHRAE Standard 55 (2013) recommended that the temperature between the head and the foot of a standing person should not exceed 3 Kelvin. To assess such local comfort it is essential to represent occupants and their surroundings in more detail

compared to what is commonly applied by default in building simulation models.

Thermo-physiological models are able to predict the human thermal state from environmental boundary conditions. Most current thermo-physiological models are derived from the model of Stolwijk et al. (1971). This was the first multi-node thermoregulatory model, dividing the human body into 25 nodes (Rupp et al. 2015). To get an accurate prediction of thermal state accurate environmental data is required as input to the physiological model. Hence, it is convenient to integrate the thermo-physiology model with environmental modelling tools, such as building performance simulation (BPS) programs. With the addition of computational fluid dynamics (CFD), BPS programs can simulate the air flow and temperature patterns within occupied spaces. A CFD-coupled BPS program can provide the physiological model with local dynamic boundary conditions, and also explicitly represent the thermal state of the occupant in the simulation. In this way the complex interaction between the human body and its thermal environment can be characterised.

Numerous attempts of coupling a thermal manikin with CFD have been described. It was widely used in the automotive industry, modelling thermal comfort in a cabin (Dixit 2015). Gan (1995) published a study using a CFD model to predict room air distribution, with Fanger's comfort model equations incorporated in the CFD model. Sorensen et al. (2002) modelled in detail the shape of a seated manikin and used it in a CFD study to calculate the radiative heat transfer coefficient and the natural convection flow around the manikin. They compared simulated and experimental results, though a

constant skin temperature was used in the simulation. Murakami et. al (2000) used Gagge's two-node model (1971) as a thermo-physiological model in a CFD study to predict the heat released from a human body. The shape of the human body was represented using a curvilinear coordinate system. Murakami stated that even though the rectangular shape was very popular to represent the shape of a human body, they believed that the physical shape of the human body could have an impact on the indoor climate.

Nielsen et al. (2003) set a CFD benchmark exercise, to validate CFD models specifically for modelling air flow around an occupant. The experimental data of the benchmark was presented in Kato and Yang (2006). This benchmark has been used by multiple researchers (Srebric et al. 2008; Deevy et al. 2008; Croper et al. 2010)

Srebric et. al (2008) studied the effects of three boundary condition elements in a CFD study; the contaminant source, the size of the body area, and the shape of the human body. They found that the fraction of convective to radiative heat flux affects the accuracy of predictions of the thermal environment around the occupant. Also, they found that using a simplified shape of human simulator will still give accurate results for the domain environment, but not when studying the local environment of the occupant, where the shape plays a major role in predicting air flow near the body. Srebric also noted that in a typical CFD approach, only the convective heat transfer is taken into account, which is insufficient where thermal radiation plays a major role of heat transfer from any heat sources. Cropper et al. (2010) published a paper on the methods used in coupling a thermo-physiology model with a commercial CFD program. In their approach they used shared files to exchange data between CFD and a thermo-physiology model. They used the Fiala model (2010), a multi-segmented human thermal model which is able to predict the response of the human body to changes in the environment, and coupled it with the ANSYS CFX commercial CFD solver.

In a more recent study Angelova et al. (2014), integrated a thermo-physiological model with the Fluent CFD software. They studied the effect of

clothing and the metabolic rate on the human body and the environment.

Many studies have linked a thermo-physiological model with a CFD simulation, some utilising advanced meshing tools and detailed manikin geometry. However, none of the research has studied the effect of such a linkage on building performance. Heat gains, as well as moisture and contaminant (e.g. CO₂) release from the occupant, are dynamic functions of the environment and the metabolic processes of the occupant. Changes in the occupant's thermal state will influence the environmental conditions of the room, potentially affecting the energy consumption of heating and ventilation systems as well as reflecting back on the occupant's thermal state. A multi-segmented thermo-physiology model explicitly simulates these processes, removing the need to represent occupants in building simulation with prescribed profiles.

By implementing a thermo-physiology model in a full BPS program, these impacts can be studied. It is important to use a multi-segmented model to predict local skin and core temperature, especially in cases of non-uniform radiant temperature.

ESP-r is a transient energy simulation system which is capable of modelling the energy and fluid flows within combined building and plant systems. The ESP-r simulation engine uses a robust numerical method to predict the building and plant energy and fluid flows. At each time-step energy and mass balance are applied for all volumes in the system, producing a differential matrix for the complete system (Clarke et al. 2007, Hand 2003).

In ESP-r a CFD domain can be associated with a thermal zone, replacing the well-mixed zone air assumption. The CFD functionality in ESP-r is strongly coupled with the building simulation, according to the conflation method developed by Beausoleil-Morrison (2000). This allows the CFD domain to intelligently configure itself according to the dynamic boundary conditions at each time step, supplied from the building domain. In turn, the CFD then passes convective fluxes at solid boundaries back to the building domain.

This paper briefly describes developments to integrate a multi-segment thermo-physiology model with ESP-r. The approach is tested with

two case studies; the displacement ventilation benchmark case of Nielsen et al. (2003) and a further case with natural ventilation.

2. METHODOLOGY

Thermo-physiology model

A multi-segmented thermo-physiology model was developed specifically for integration with ESP-r. The model is based on the AUB bioheat model developed by Salloum et al. (2006), and constitutes a passive and an active system. The passive system simulates the heat transfer between the body segments and the environment through convection, radiation, conduction and evaporation. The active system solves all physiological variations as the shivering, sweating and blood flow. The model is based on realistic anatomical data of the human body. The blood circulation system in the model takes the pulsatile blood flow into consideration, and calculates the perfusion flow rates in the core and skin nodes. It describes and simulates the arterial system by using the multi-branched model of the human arterial system of Avolio (Salloum et al. 2013). The model consists of 25 body segments, and each segment is represented by four concentric layers (nodes) core, skin, artery and vein. Superficial veins are considered at the limbs (Salloum et al. 2007, Karki et al. 2013).

Integration with ESP-r

Figure 1 represents the coupling method and the data exchange between the solvers at every time step.

In an ESP-r CFD domain blockages can be defined to represent solid objects which block air flow. These are used to construct a manikin representing a human body, with a separate blockage defined for the head, torso, and all four limbs (6 in total). The constraint of orthogonal gridding in ESP-r necessitates representation of the occupant body shape in a rectangular form. Convective heat loads for each body segment are evenly distributed over its surface area within the CFD domain. Radiative loads are treated as shortwave radiation impinging on the interior surfaces of the room in the building domain. The latent load and moisture release are implemented as a vapour source in the CFD cell in front of the face.

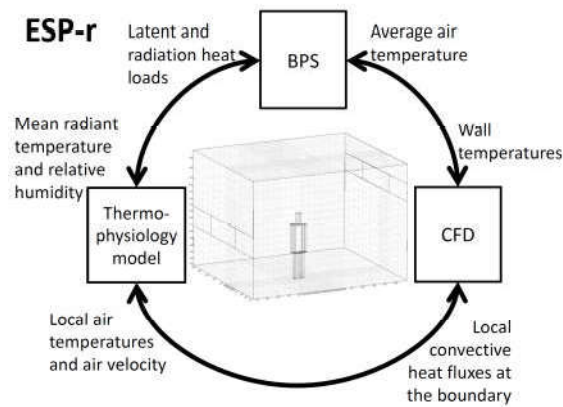


Figure 1: Coupling representation.

The user must define the number of occupants, and the gender, the metabolic rate and clothing of each in the corresponding zone. This replaces the prescription of occupant heat gains required previously, and uses the same schedule-based syntax. In this way users can prescribe the presence and activity of occupants varying through time.

Simulation parameters

The CFD in ESP-r uses a finite volume method. In both case studies, the adaptive conflation controller (ACC) developed by Beausoleil-Morrison (2000) was activated, which manages interactions between the building and CFD modelling domains. The defacto standard $k-\epsilon$ mode turbulence model was used in the simulations. Buoyancy was modelled using the Boussinesq approximation with a reference temperature of 24°C. The convergence criterion was a maximum residual value 10^{-3} .

Simulations were performed with 2 time steps per hour, on a computer with an Ubuntu operating system with 6 GB RAM and a 3.60 GHz CPU.

3. CASE STUDIES

Two simulation cases were considered. Firstly, for the purpose of validation the benchmark of a displacement ventilation case from Nielsen et al. (2003) was simulated and compared with experimental data gathered by Kato and Yang (2006) measuring the flow field around a manikin. Secondly, to demonstrate the transient coupling capability, a case with natural ventilation was simulated.

Displacement ventilation benchmark case

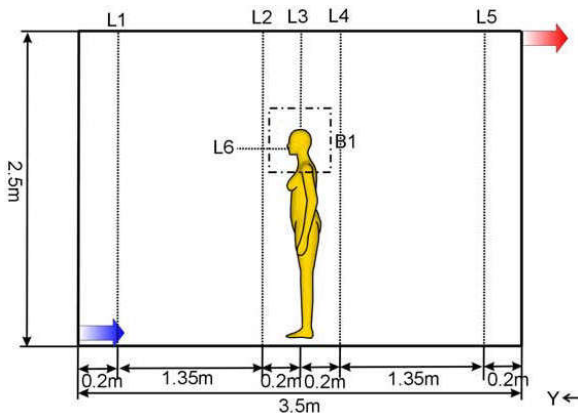


Figure 2: Sketch of the benchmark vertical measuring pole (Nielsen et al. 2003)

This case study sought to reproduce the benchmark described by Nielsen et al. (2003). The room has dimensions 3m width x 3.5m depth x 2.5m height, has an inlet in the bottom of the east wall with dimensions 0.2x0.4m and an outlet in the top of the opposite wall of 0.3x0.3m. The boundary conditions of air entering the room were 21.8°C inlet temperature and average velocity of 0.182m/s. The measurements of air velocity and temperature were made at various locations; four vertical poles were set, two in front of the manikin and two behind it. The temperature was measured at seven different heights while velocity was taken at six different heights. The velocity above the head was also monitored by using the particle image velocity (PIV). Figure 2 shows the vertical measuring pole position with dimension used in the benchmark, the supply and exhaust openings marked, and a manikin placed in the middle of the room. Figure 3 illustrates the computational domain of the benchmark in ESP-r, showing the inlet and outlet openings and the manikin in the middle of the room.

The benchmark set a sensible heat load from the manikin of 76W, though the radiant/conductive fraction is not mentioned. Walls are considered adiabatic in the benchmark which could have some implication on results, as heat transfer from walls typically has a significant effect on room air flow.

The CFD domain grid consisted of a rectangular structured mesh with cell dimensions approximately 0.03m around the human body and about 0.1m in other regions of the room. As described in section 2, the body geometry was

represented by six cuboidal blockages representing the head, torso, and all four limbs. The total number of cells was 81,000.

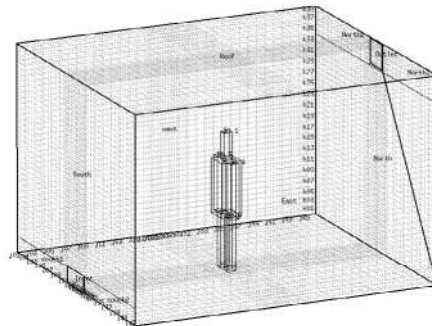


Figure 3: CFD domain in ESP-r

Table 1 shows the body part surface area used for this simulation.

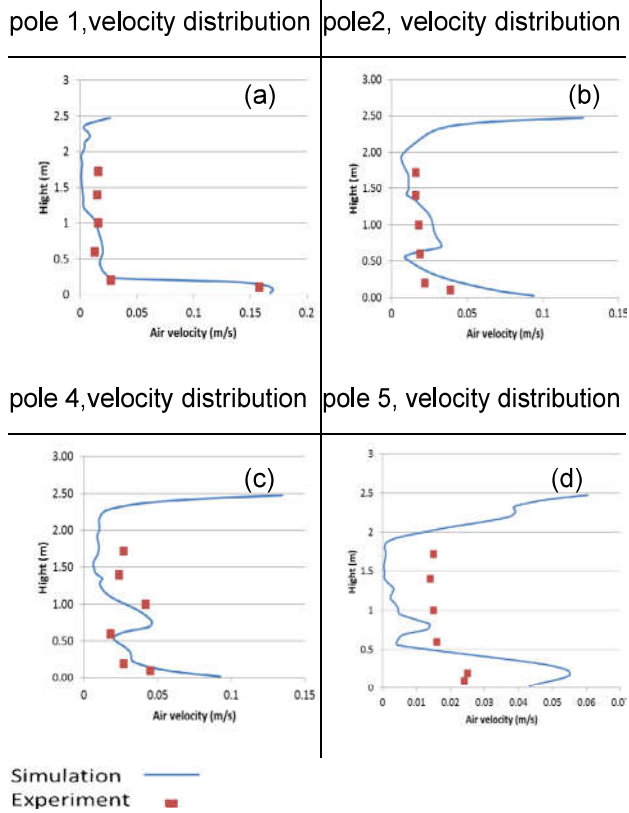
Table 1 Manikin body surface area used in simulation

Body Part	Area in m^2
Head	0.1224
Trunk	0.5984
One Arm	0.2448
One Leg	0.306
Total	1.8224

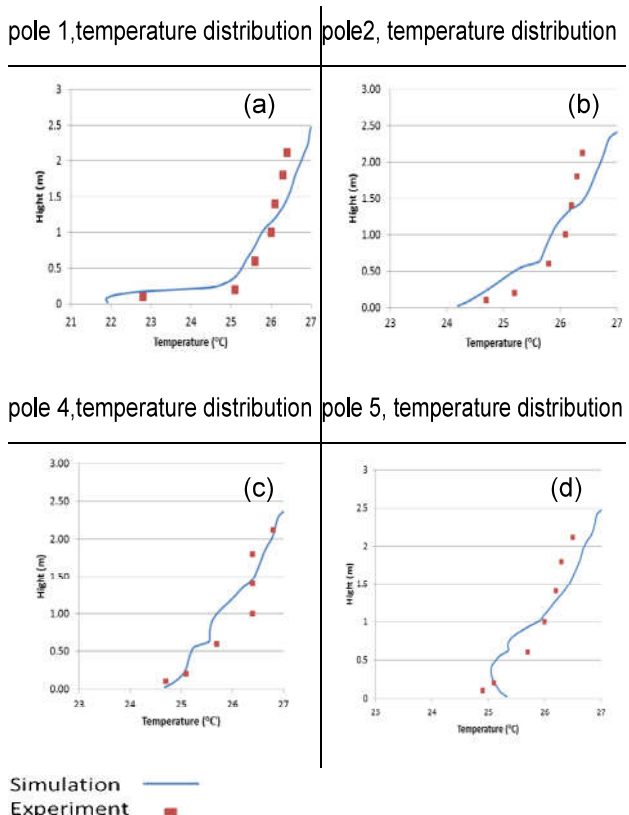
Results

The description of the experimental data, published by Kato and Yang (2006), did not provide any accuracy or measurement error to be considered in our comparison. For this reason a qualitative comparison between the experimental and simulated results of both air velocity and temperature of the four poles has been done.

Figures 4 a, b, c and d shows the measured and simulated air velocity results for the different locations and heights. Figures 5 a, b, c and d shows the air temperature in front and behind the manikin for the different heights. In order to evaluate the accuracy of numerical results the root mean square (RMS) residuals were calculated for each pole, according to equation 1, where Y is the considered data air temperature or velocity and n is the number of data. Maximum RMS was 0.68 °C for temperature and 0.025 m/s for velocity, table 2 shows the temperature and velocity RMS values for each pole.



Figures 4 a,b,c,d: Plots of the simulation vs. experimental results of velocity for poles 1,2,4,5 respectively.



Figures 5 a,b,c,d: Plots of the simulation vs. experimental results of temperature for poles 1,2,4,5 respectively.

Table 2 Temperature and velocity RMS values for each pole

RMS	Pole1	Pole2	Pole4	Pole5
Temperature	0.683	0.342	0.313	0.50
Velocity	0.025	0.016	0.012	0.018

$$RMS = \sqrt{\frac{\sum_{i=1}^n (Y_{exp,i} - Y_{sim,i})^2}{n}} \quad (1)$$

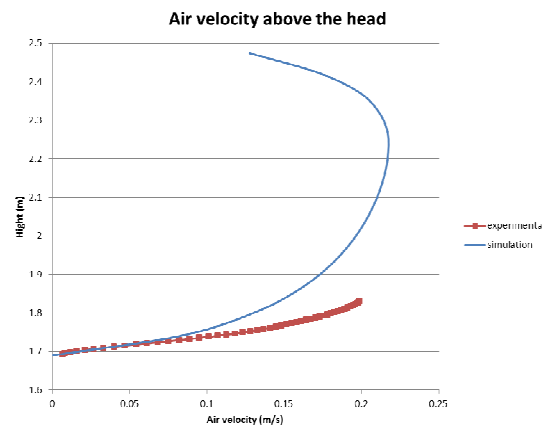


Figure 6: Simulated vs. experimental results of air velocity above the head.

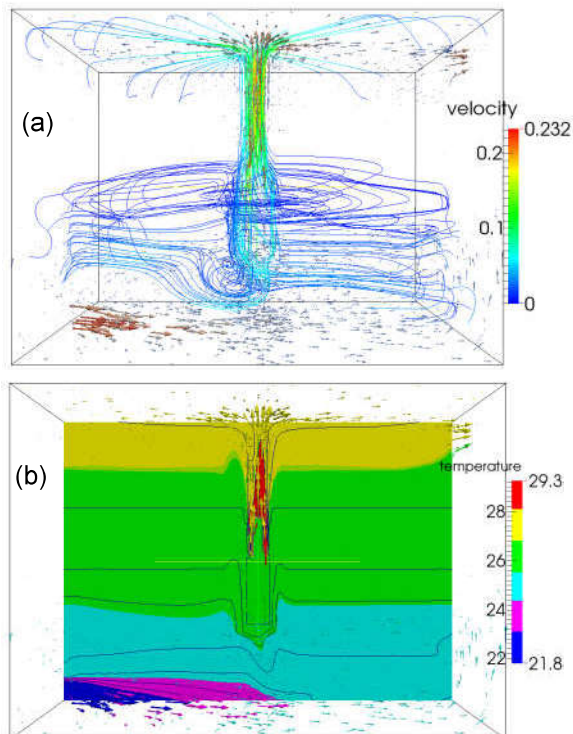


Figure 7 a,b: Air velocity and temperature distribution across the middle of y axis.

Figure 6 shows the differences in the air velocity above the head between the simulated and experimental results. Air velocity in the simulated results reached 0.2 m/s around 10 cm higher compared to the experimental results. This difference in the results could be because of the simplified rectangular shape of the head.

Figure 7a shows velocity stream lines and 7b the temperature distribution of a cross section in the middle of the Y axis, through the inlet, outlet and manikin.

Natural ventilation case

CFD domain geometry is shown in figure 8. The room model has dimensions 4.2m width x 3.6m depth x 3m height. It includes a large opening located high in the East wall exposed to the external environment, and another opening low in the West wall internal partition (attached to another zone);. Weather data for a slightly warm day was chosen for this case study as it was considered acceptable for a natural ventilation case. The simulation period was an assumed office working day, from 08:00 in the morning until 19:00 evening. The gridding mesh consisted of 10,080 cells. The manikin was located in the middle of the room. Table 3 shows the weather data chosen for three hours of the simulation to show the variation.

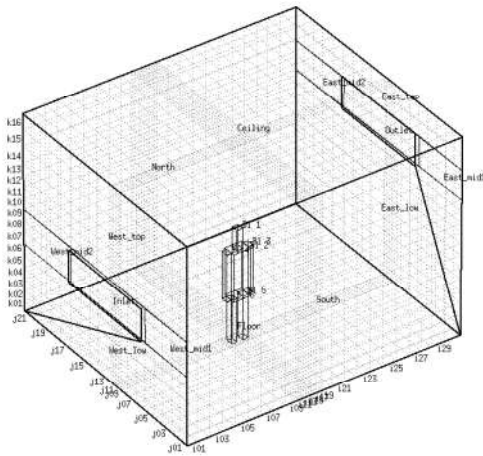


Figure 8: Representation of occupant inside a naturally ventilated domain.

The occupant was given an initial metabolic rate of 1.4 met (standing doing light industrial work), changing to 2.4 met between 12:00 and 13:00 and then back to 1.4 met until the end of the simulation day. This approach demonstrated the effect of variable metabolic rate during a transient simulation. Clothing level was chosen

as a summer clothes ensemble with insulation 0.45 clo (clothing layers covering thighs, chest and upper arms).

Table 3: Weather data for each hour of the simulation time for the simulation date.

Hour	Temperature	wind velocity m/s	wind direction	relative humidity
12	25	2.1	10	39
13	25.7	4.1	70	35
14	26.4	5.1	10	38

Results

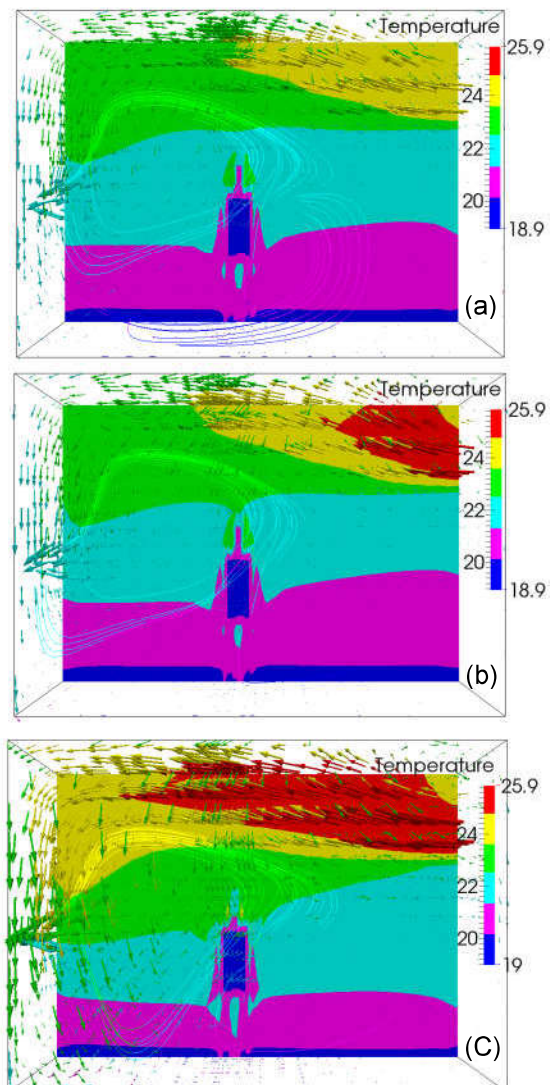


Figure 9 a, b, c: Temperature distribution around the manikin at a) 12:00 b) 13:00 c) 14:00

Figures 9 a, b and c gives results visualisations for temperature distribution at times 12:00 13:00 and 14:00 respectively. Temperature on a plane bisecting the occupant and the air flow openings, and arrow representations of the flow field (scaled by velocity), are shown. It can be seen how the air velocity change at the inlet opening corresponds to the weather data.

Figure 10 a shows the variation in heat loss from the dynamic occupant over the simulation period. Transient variation in sensible and latent loads can be clearly seen as a result of the varying metabolic rate. In addition figure 10 b shows the skin temperature of the occupant body parts and the overall temperature. From the graph we can see the variation of the skin temperature over the simulation time; these temperatures can be used as input for a thermal sensation and comfort model.

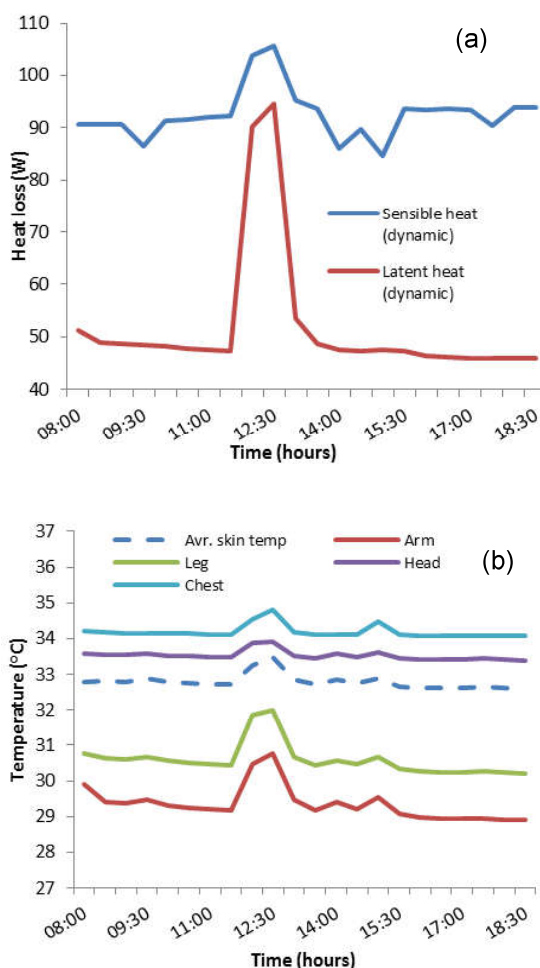


Figure 10 a,b: Variation of total sensible and latent heat during the simulation time; b) surface temperature of each body part.

Conclusions

In this study we have briefly presented the coupling method of a multi-segmented thermophysiology model with ESP-r and its integrated CFD solver. The coupling method was validated using a benchmark study with displacement ventilation and our results were in a good agreement with the published data. The transient occupant representation of the coupling approach was also demonstrated in a natural ventilation case study.

The new functionality demonstrated in this paper enables improved modelling of occupants and their thermal interaction with the building in

ESP-r. This removes the need to prescribe profiles such as occupant heat gains, as this is modelled explicitly as a function of prescribed occupant activity and environmental conditions.

Further work on the coupling method and studies on thermal comfort adaptation for multiple manikins with different thermal behaviour in the same domain will be presented later. The approach can also be used to investigate how the thermo-physical model affects building model performance.

Reference

- American Society of Heating, Refrigerating and Air-Conditioning Engineers (ASHRAE) (2013) Standard 55 - Thermal environmental conditions for human occupancy (Atlanta, GA).
- Angelova RA, et al.(20015) . CFD Based Study of Thermal Sensation of Occupants Using Thermophysiological Model. Part II: Effect of metabolic rate and clothing insulation on human-environmental interaction. *Int J Cloth Sci Tech* 27(1): 60-74.
- Beausoleil-Morrison, I. (2000) The Adaptive Coupling of Heat and Air Flow Modelling within Dynamic Whole-Building Simulation, PhD thesis, University of Strathclyde, Glasgow.
- Bourgeois D. et al. (2004) Adding sub-hourly occupancy prediction, occupancy-sensing control and manual environmental control to ESP-r, in Proceeding of Esim 2004, Vancouver, BC, 2004, pp. 119– 126
- Bolineni S, van Treeck C, Stratbucker S (2014). Coupling strategy for transient simulation of

- human thermoregulation and CFD indoor airflow models. In: Proceedings of 13th International Conference on Indoor Air Quality and Climate, Hong Kong, China.
- Clarke J. A., Kelly N. J & Tang D. (2007) A Review of ESP-r's Flexible Solution Approach and its Application to Prospective Technical Domain Developments, Advances in Building Energy Research, 1:1, 227-247.
- Cropper PC, et al. (2010). Coupling a model of human thermoregulation with computational fluid dynamics for predicting human–environment interaction. *Journal of Building Performance Simulation*, 3: 233–243.
- Cook M, et al. (2013). Coupled CFD and thermal comfort modeling in cross-ventilated classrooms. In: Proceedings of ASHRAE Annual Conference, Denver, USA.
- Cropper P, et al. (2008). Exchange of simulation data between cfd programmes and a multisegmented human thermal comfort model. In: Proceedings of Air Conditioning and the Low Carbon Cooling Challenge, Windsor, UK.
- Fiala, D. et al. (2001) Computer prediction of human thermoregulatory and temperature responses to a wide range of environmental conditions. *Int. J. Biometeorol.*, 45: 143-159
- Gagge AP et al.(1971) An Effective Temperature Scale Based on a Simple Model of Human Physiological Regulatory Response. *ASHRAE Transactions.*;77:247-262.
- Gan, G. (1995) Evaluation of room air distribution systems using computational fluid dynamics, *Energ. Buildings*, 23, 83–93.
- Gao NP, Niu JL (2005). CFD study of the thermal environment around a human body: A review. *Journal of Indoor Built Environment*, 14: 5–16.
- Hand, J. (2003) The ESP-Cookbook. ESRU Publications: University of Strathclyde, Glasgow,
- Karaki W., Ghaddar N., Ghali K., Kuklane K., Holmer I., Vanggaard L., (2013) Human thermal response with improved AVA modeling of the digits, *Int. J. Therm. Sci.* 67 41e52.
- Murakami S, Kato S, Zeng J (1995) Development of a computational thermal manikin—CFD analysis of thermal environment around human body. In: Proceedings of Tsinghua HVAC'95, Beijing, China, Vol. 2, pp. 349–354.
- Nielsen PV, Murakami S, Kato S, Topp C, Yang JH. Benchmark tests for a computer simulated person. Project report. Denmark: Aalborg University, 2003. p. 7.
- Salloum M, Ghaddar N, Ghali K. (2007) A new transient bioheat model of the human body and its integration to clothing models. *International Journal of Thermal Sciences*;46(4):371e84.
- Sørensen D.N., Voigt L.K. (2003), Modeling flow and heat transfer around a seated human body by computational dynamics. *Building and Environment*, 38 pp. 753-762
- Srebric J, Vukovic V, He G, Yang X, (2008) CFD boundary conditions for contaminant dispersion, heat transfer and airflow simulations around human occupants in indoor environments, *Building and Environment* 43 (3) 294–303.